

Aging under shear: Structural relaxation of a non-Newtonian fluid

R. Di Leonardo,^{1,*} F. Ianni,^{1,2} and G. Ruocco^{1,2}

¹*INFN-CRS SOFT, c/o Università di Roma "La Sapienza," I-00185 Roma, Italy*

²*Dipartimento di Fisica, Università di Roma "La Sapienza," I-00185 Roma, Italy*

(Received 14 June 2004; revised manuscript received 3 November 2004; published 18 January 2005)

The influence of an applied shear field on the dynamics of an aging colloidal suspension has been investigated by the dynamic light-scattering determination of the density autocorrelation function. Though a stationary state is never observed, the slow dynamics crosses between two different nonequilibrium regimes as soon as the structural relaxation time τ_s approaches the inverse shear rate $\dot{\gamma}^{-1}$. In the shear-dominated regime (at high $\dot{\gamma}$ values) the structural relaxation time is found to be strongly sensitive to the shear rate ($\tau_s \sim \dot{\gamma}^{-\alpha}$, with $\alpha \sim 1$) while aging proceeds at a very slow rate. The effect of the shear on the detailed shape of the density autocorrelation function is quantitatively described, assuming that the structural relaxation process arises from the heterogeneous superposition of many relaxing units, each one independently coupled to shear with a parallel composition rule for time scales: $1/\tau \rightarrow 1/\tau + A\dot{\gamma}$.

DOI: 10.1103/PhysRevE.71.011505

PACS number(s): 64.70.Pf, 82.70.-y, 83.60.Fg

One of the most peculiar and intriguing behaviors of soft materials is the strong sensitivity of their flow properties to the application of an even slight external deformation [1]. When a liquid flows in a steady shear state, the inverse shear rate $\dot{\gamma}^{-1}$ introduces a new relevant time scale in the dynamics. On a microscopic level a non-Newtonian character reflects a competition between $\dot{\gamma}^{-1}$ and the natural time scale of those particle rearrangements controlling the macroscopic flow properties. For moderate shear rates, i.e., those occurring in the macroscopic world, mainly the slow modes are affected by the shear and give rise to complex rheological behavior. Understanding the physical mechanism governing the interaction between slow dynamics and shear has been the subject of great theoretical and numerical efforts in recent years.

On the theoretical side, some of the most powerful tools for the investigation of slow dynamics in complex systems, such as mode coupling theory [2,3], mean-field models [4–7], trap models [8,9], and molecular dynamics simulations [10–12], have been recently extended to account for the presence of driving forces. The general picture emerging from these studies indicates that the structural dynamics is very sensitive to even moderate shear rates whenever $\dot{\gamma}^{-1}$ becomes of the same order of the characteristic time scale for structural rearrangements. In particular, even starting from nonequilibrium, aging states, the presence of shear ensures the existence of a stationary state whose correlation functions decay to zero on a time scale governed by $\dot{\gamma}^{-1}$.

Despite the growing amount of numerical and theoretical work investigating the shear-influenced slow dynamics, an experimental microscopic counterpart is still relatively poor. Evidences for a shear-dependent structural relaxation time have been obtained by diffusing wave spectroscopy (DWS) [13,14] and light scattering echo experiments (LSE) [15]. Shear flow is found to deeply influence dynamics not only by rejuvenating old samples [13,14] but also amplifying aging

when a low-amplitude oscillation is applied (overaging) [14].

Unfortunately the statistical properties of multiple scattered light (probed in DWS and LSE experiments) are not easily represented in terms of the particles' correlation functions. No attempt has been made up to now to investigate shear-influenced dynamics using dynamic light scattering (DLS) in the single-scattering regime. Such a technique directly probes the intermediate scattering function of the colloidal particles $F_q(t)$, which plays a central role in both theoretical and numerical approaches.

In this paper, we investigate the evolution of the density autocorrelation function of an aging colloidal suspension subject to a steady shear flow. The competition between the structural relaxation time and the inverse shear rate gives rise to a complex dynamical behavior that we could quantitatively analyze by studying the detailed shape of the particles' density autocorrelation function. The sample is an aqueous suspension of Laponite, a highly thixotropic liquid that undergoes structural arrest on a time scale that strongly depends on concentration and ionic strength [16], and that can be as long as few months [17]. We found that the aging dynamics displays two different regimes whose boundary is marked by the condition $\tau_s \dot{\gamma} \sim 1$. As long as the characteristic relaxation time τ_s is small on the time scale $\dot{\gamma}^{-1}$, aging is unaffected by the presence of shear. During aging, dynamics slows down, and when τ_s becomes of the order of $\dot{\gamma}$, the system enters a shear-dominated regime where aging is strongly reduced and the structural relaxation time is very sensitive to $\dot{\gamma}$. The intermediate-scattering functions, characterizing the slow nonequilibrium dynamics of the sheared sample, are well described, assuming an heterogeneous scenario where the complex dynamics results from the superposition of relaxing units, each one independently coupled to the shear rate with a parallel composition rule for time scales: $1/\tau \rightarrow 1/\tau + A\dot{\gamma}$.

The system consists of an aqueous suspension of Laponite, a synthetic-layered silicate provided by Laporte Ltd. Particles are disk shaped with a diameter of 25 nm and 1 nm thickness. Laponite powder is dispersed in ultrapure water at

*Electronic address: roberto.dileonardo@phys.uniroma1.it

3% wt concentration and stirred for ~ 30 min. The obtained suspension, which is optically transparent and initially liquid, is loaded into a homemade, expressly designed, cone and plate shear cell having a flat optical window as the static plate. Cell loading (through a Millipore Millex-AA 0.45 μm filter) is taken as the origin of waiting times. Incident laser beam (He-Ne, 10 mW) and scattered light pass through the same optical window. The scattered light is collected by a monomode optical fiber, detected by a photomultiplier and analyzed by a homemade software correlator, after being optionally mixed with a coherent local oscillator field. The scattering geometry is fixed (scattering vector $q=25 \mu\text{m}^{-1}$). The possibility of choosing a heterodyne correlation scheme enables direct access to the detailed velocity profile in the shear cell. Wall slip and distortion from linearity in the velocity profile are found to be negligible in the whole shear rate range here investigated. The nonequilibrium dynamics of Laponite suspensions flowing in a “steady” shear state is then constantly monitored through the normalized intensity autocorrelation function $g^{(2)}(t_w, t) = \langle I(q, t_w)I(q, t_w + t) \rangle / \langle I(q, t_w) \rangle^2$, where $\langle \cdot \rangle$ indicates the temporal average over the acquisition time T , which is always much longer than the characteristic slow relaxation time τ ($T/\tau \geq 10^2$), but also much shorter than the time one should wait before changes in τ are significant ($T \partial \ln \tau / \partial t_w \leq 10^{-2}$). In the single-scattering regime and within the Gaussian approximation $g^{(2)}(t_w, t) = 1 + |F_q(t_w, t)|^2$ [18], where $F_q(t_w, t) = \langle \rho_{-q}(t_w) \rho_q(t_w + t) \rangle / \langle \rho_{-q}(t_w) \rho_q(t_w) \rangle$ is the intermediate-scattering function of the colloidal particles. In order to avoid purely geometric decorrelation of scattered light, due to both advection and transit time effects [19], steady shearing is interrupted every 10 min and the correlation functions are collected in short (few tens of seconds) time intervals during which the rotor is stopped ($\dot{\gamma}=0$). The robustness of the results with respect to changes in acquisition protocol has been checked.

The top frame of Fig. 1 shows the evolution of $g^{(2)}(t_w, t)$, in the absence of shear, for an evenly spaced set of waiting times t_w spanning the interval 0.1–15 hours. As already observed in [21], aging dynamics displays a two-step relaxation scenario: (i) a fast exponential relaxation process related to single particle diffusion and whose characteristic time τ_f (20–40 μs) remains of the same order of magnitude found in very dilute suspensions [22] and (ii) a slow stretched exponential process related to cooperative motions [23] and whose characteristic time τ_s grows exponentially fast with waiting time t_w while becoming strongly stretched (stretching parameter β down to 0.2). In the bottom frame of Fig. 1, we reported the evolution of $g^{(2)}(t_w, t)$, observed on the same set of t_w reported in top frame, when a shear rate $\dot{\gamma} = 223 \text{ s}^{-1}$ is applied. Though a stationary state is never reached in the observation time window, for long enough waiting times, the slow relaxation time grows slower than exponentially (the correlation functions come closer), while the shape of the relaxation function approaches a constant profile (constant stretching exponent). The two-step decay for $F_q(t_w, t)$

$$F_q(t_w, t) = f \exp[-(t/\tau_s)^\beta] + (1-f) \exp[-t/\tau_f],$$

where all parameters (f, τ_s, β, τ_f) depend on t_w and on q provides a very good fit for all the correlators corresponding to

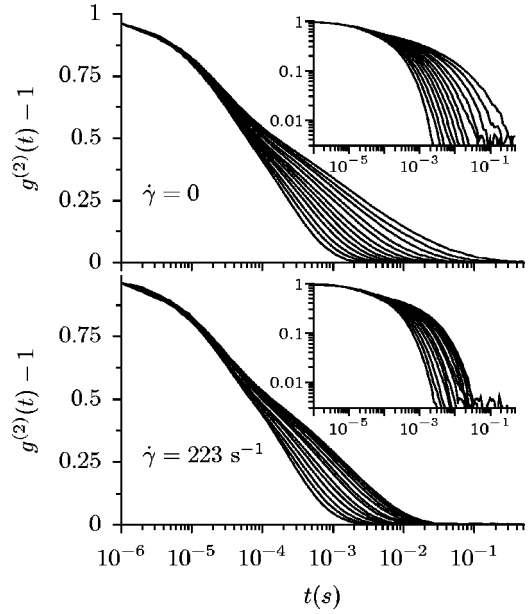


FIG. 1. Normalized intensity autocorrelation function for ten equally spaced waiting times between 0.1 and 15 hours. The top frame refers to aging without shear, while the bottom frame refers to aging under shear with $\dot{\gamma}=223 \text{ s}^{-1}$. Inset plots show the same data in a double-logarithmic scale.

the different $\dot{\gamma}, t_w$ values here investigated. The presence of a shear-induced crossover becomes more evident if we plot the fitting parameters $\langle \tau_s \rangle$ (average slow relaxation time $\langle \tau_s \rangle = \int_0^\infty \exp[-(t/\tau_s)^\beta] dt = \tau_s / \beta \Gamma(1/\beta)$, where Γ is the Euler gamma function) and β (stretching exponent), as a function of t_w for different shear rates as in Fig. 2.

As long as the system’s dynamics is fast on the time scale $\dot{\gamma}^{-1}$ (indicated by arrows in the plot), nonequilibrium dynamics takes place as if shear were not present—both the relaxation time τ_s and the corresponding stretching exponent β evolve with waiting time following the $\dot{\gamma}=0$ curve (full circles). The presence of shear starts to affect the dynamics as soon as τ_s becomes larger than $\dot{\gamma}^{-1}$: the growth of τ_s is dramatically reduced (even if not completely stopped) and the stretching parameter β behavior flattens. In the shear-dominated region, $\langle \tau_s \rangle$ displays a power-law dependence on t_w (as evidenced in the double-logarithmic plot inserted in the top panel of Fig. 2) with an exponent that is roughly one for the higher shear rate and increases above unity for lower shear rates. Though aging is never completely absent, the slow relaxation dynamics, for a given waiting time, appears to be very sensitive to $\dot{\gamma}$ being faster and less stretched as $\dot{\gamma}$ increases. If we suddenly increase $\dot{\gamma}$, rejuvenation is observed, leading to a faster relaxation time and a smaller stretching (higher β). Crosses in Fig. 2 are the average relaxation times and stretching exponents of two rejuvenated samples obtained by the two subsequent shear rate jumps: $63 \text{ s}^{-1} \rightarrow 223 \text{ s}^{-1}$ and $223 \text{ s}^{-1} \rightarrow 446 \text{ s}^{-1}$. We want to stress here that the exponential increase of the slow relaxation time $\tau_s \sim \tau_0 \exp[-t_w/\tau_a]$ reveals the presence of at least two well-separated intrinsic time scales (τ_a and τ_s) characterizing the aging dynamics of Laponite. Nevertheless, though the shear rate is always such that $\dot{\gamma}\tau_a \gg 1$, aging dynamics is only af-

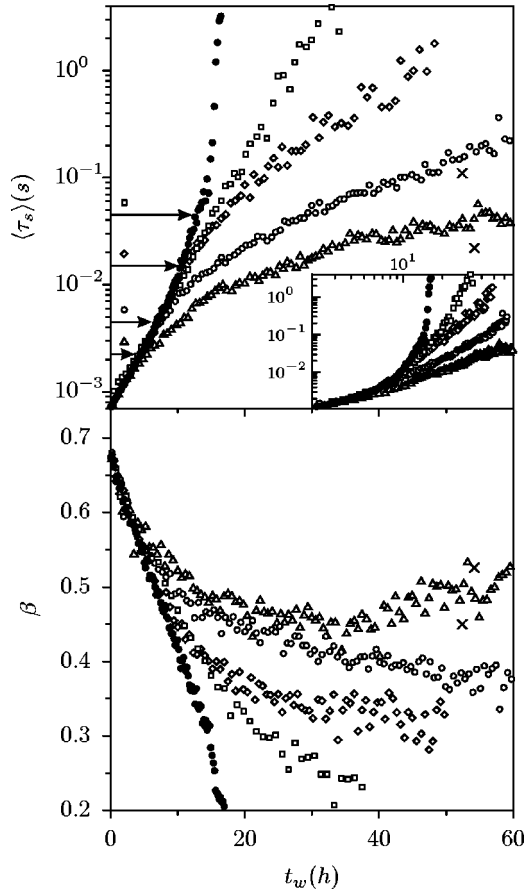


FIG. 2. Average slow relaxation time $\langle \tau_s \rangle$ and stretching exponent β as a function of waiting time t_w during aging under different shear rates $\dot{\gamma}$: (Δ) 446, (\circ) 223, (\diamond) 67, (\square) 22 s $^{-1}$. The solid symbols (\bullet) refer to aging without shear. The arrows in top frame indicate the $\dot{\gamma}^{-1}$ values corresponding to each curve. The inset in the top frame shows the same data in a double-logarithmic scale.

ected by shear when the condition $\dot{\gamma}\tau_s \sim 1$ is reached. As already reported in [13,14] shear is found to have a deep effect on aging dynamics. Here we can directly access through $F_q(t)$ the particles' dynamics resulting from the competition between the highly stretched structural relaxation and the inverse shear rate time scale. In particular, we found that $\dot{\gamma}\tau_s \sim 1$ marks a crossover between an unperturbed and a “shear-dominated” aging.

This is highlighted in Fig. 3 where we reported the values of $\langle \tau_s(\dot{\gamma}, t_w) \rangle$ for constant t_w as a function of $\dot{\gamma}$. The gray region represents the half plane $\langle \tau_s \rangle < \dot{\gamma}^{-1}$ where slow dynamics takes place on a time scale shorter than $\dot{\gamma}^{-1}$. This region is not affected by the presence of shear: the fluid is Newtonian and, similarly to viscosity, $\langle \tau_s \rangle$ is not dependent on $\dot{\gamma}$. On the other hand, shear plays an important role in the complementary half plane where $\langle \tau_s \rangle$ displays a strong sensitivity to $\dot{\gamma}$. The non-Newtonian behavior in the upper half plane of Fig. 3 resembles the same $\dot{\gamma}^{-1}$ power law (dashed line) observed in rheological measurements of Laponite viscosity [13].

The whole scenario depicted above provides a microscopic counterpart of the strong shear-thinning behavior ob-

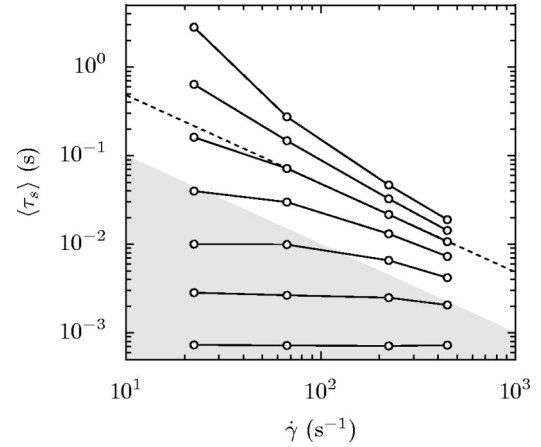


FIG. 3. Average slow relaxation time $\langle \tau_s \rangle$ as a function of shear rate $\dot{\gamma}$ for seven evenly spaced waiting times between 0 and 30 h. The gray area represents the half plane $\langle \tau_s \rangle < \dot{\gamma}^{-1}$. The dashed line is a fit to a $\dot{\gamma}^{-1}$ power law.

served in rheological studies of Laponite [13] and of many other soft materials. In both real [1] and simulated [10,11] liquids, the viscosity crossover from a Newtonian to a non-Newtonian regime (power-law dependence on $\dot{\gamma}$), is usually found to be described by scaling laws such as

$$\eta(\dot{\gamma}) \simeq \frac{\eta(0)}{1 + \dot{\gamma}\tau_\eta}. \quad (1)$$

Since viscosity is related to structural relaxation, one could think, as suggested in [10], of a dynamical analog of (1) in the form

$$\frac{1}{\tau(\dot{\gamma})} \simeq \frac{1}{\tau(0)} + A\dot{\gamma}, \quad (2)$$

which has also the advantage of an easily readable meaning: shear rate provides a parallel relaxation channel to the system that becomes predominant as soon as $1/\tau(0, T) \ll A\dot{\gamma}$. This simple relation is indeed found to work remarkably well in computer models for supercooled liquids [10]. Using the same kind of reasoning, one would expect that even in an aging sample, as soon as the unperturbed relaxation time grows large enough, shear rate will fix the relevant time scale and the system will become stationary even in the non-ergodic phases. This is actually what has been observed in a number of recent numerical and theoretical papers, and also by rheological studies.

We are now in the position of testing (2) by directly investigating the complete time behavior of density dynamics in the presence of a shear flow. At a first glance one would conclude that Fig. 2 is in contradiction with (2) and the expectation that shear stops aging. It is, in fact, evident that the relaxation time continues to grow, even if no longer exponentially fast, at least for more than one order of magnitude after it first “feels” the shear field. On the other hand, as shown in Fig. 2, when the crossover occurs, the value of the stretching exponent is about 0.5 or less. This means that the unperturbed dynamics occurs on a broad spectrum of time scales (spanning two decades at least) and that $\langle \tau_s \rangle$ only rep-

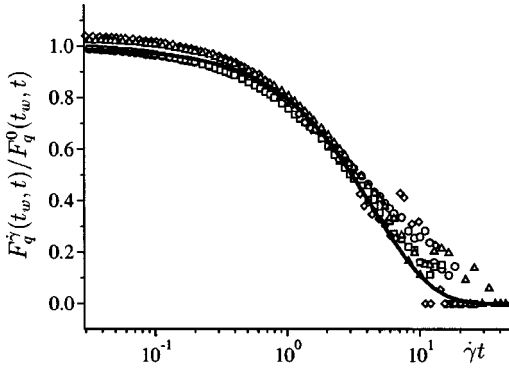


FIG. 4. Ratio $F_q^\gamma(t_w, t)/F_q^0(t_w, t)$ as a function of $\dot{\gamma}t$, where $F_q^\gamma(t_w, t)$ is the intermediate scattering function measured after a waiting time t_w during aging with applied shear rate $\dot{\gamma}$. \circ , $\dot{\gamma} = 446 \text{ s}^{-1}$, $t_w = 10 \text{ h}$; \square , $\dot{\gamma} = 446 \text{ s}^{-1}$, $t_w = 14 \text{ h}$; \triangle , $\dot{\gamma} = 223 \text{ s}^{-1}$, $t_w = 14 \text{ h}$; \diamond , $\dot{\gamma} = 67 \text{ s}^{-1}$, $t_w = 14 \text{ h}$. The solid line is an exponential fit $\exp[-A\dot{\gamma}t]w$.

resents an average relaxation time. Many approaches to slow dynamics in complex systems [20] suggest that such a broad spectrum of time scale arises from the heterogeneous character of slow dynamics. Assuming this heterogeneous scenario, shear is only effective in interrupting aging for those time scales growing longer than a fixed, shear-dependent cut-off. In other words, we expect that (2) holds separately for every time scale composing structural relaxation. The above scenario qualitatively accounts for both the observations of a slowly growing (nonsaturating) structural relaxation time after the crossover and a narrowing in the distribution of time scales with respect to the unperturbed case. We want to push now the above observations on a more quantitative ground. Assuming that (2) holds separately for each time scale and calling $G(t_w, \tau)$ the unperturbed distribution of time scales,

$$F_q^0(t_w, t) = \int_0^\infty G(t_w, \tau) \exp[-t/\tau] d\tau, \quad (3)$$

we would expect that shear affects (3) as follows:

$$F_q^\gamma(t_w, t) = \int_0^\infty G(t_w, \tau) \exp[-t(1/\tau + A\dot{\gamma})] d\tau \quad (4)$$

$$= F_q^0(t_w, t) \exp[-tA\dot{\gamma}]. \quad (5)$$

In other words, if we divide the correlation function measured at a given waiting time t_w and shear rate $\dot{\gamma}$ by the corresponding unperturbed ($\dot{\gamma}=0$) correlation measured at the same t_w and plot the result as a function of $\dot{\gamma}t$, we should obtain the master curve $\exp[-A\dot{\gamma}t]$.

In Fig. 4 we report the result of such a procedure obtained for three different values of $\dot{\gamma}$ and two waiting times. All curves collapse on the same master curve, which is well

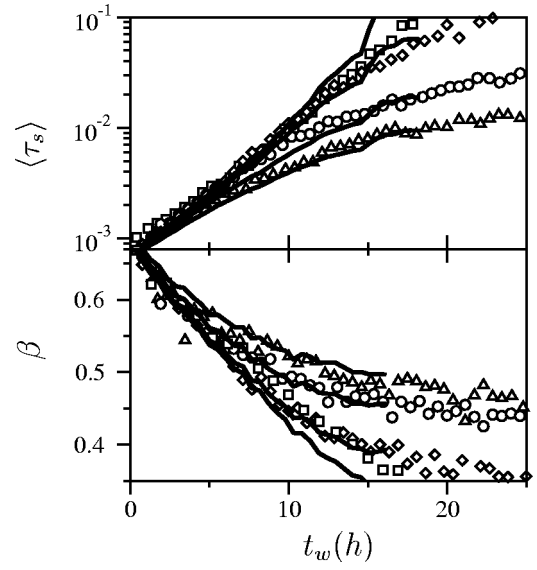


FIG. 5. Average relaxation time (top frame) and the stretching parameter (bottom frame) as a function of waiting time for different applied shear rates. The symbols are data in Fig. 2; the solid line is the prediction of the phenomenological model described in the text.

represented by a simple exponential with $A=0.22$ (solid line). Similarly, we could predict the shape of relaxation for given t_w and $\dot{\gamma}$ by simply multiplying the unperturbed correlation function for the same t_w by the function $\exp[-A\dot{\gamma}t]$. If we do this for the $\dot{\gamma}$ values here investigated and fit the result with a stretched exponential, we obtain a prediction for $\tau_s(t_w, \dot{\gamma})$ and $\beta(t_w, \dot{\gamma})$.

The results of such a procedure, for those t_w values where $F_q^0(t_w, t)$ is available, are shown in Fig. 5 as solid lines. The overall agreement with the directly measured data points (open symbols) is very satisfactory and supports the picture of the slow nonequilibrium dynamics of Laponite as a heterogeneous superposition of relaxing units each independently coupled to shear.

In conclusion, we investigated the effect of shear on the nonequilibrium structural dynamics of an aging colloidal suspension of Laponite. The presence of a shear flow strongly affects dynamics as soon as structural relaxation enters the time scale $\dot{\gamma}^{-1}$. In this shear-dominated region, the shear-rate dependence of the average slow relaxation time $\langle\tau_s\rangle$ is well approximated by the power law $\dot{\gamma}^{-\alpha}$ with $\alpha \sim 1$. The effect of shear on the detailed shape of the intermediate scattering function can be well described assuming that the slow relaxation process arises from the heterogeneous superposition of many relaxing units each one independently coupled to shear rate with a parallel composition rule for time scales: $1/\tau \rightarrow 1/\tau + A\dot{\gamma}$.

The authors wish to thank F. Zamponi for helpful discussions.

- [1] R. G. Larson, *The Structure and Rheology of Complex Fluids* (Oxford University Press, Oxford, 1999).
- [2] M. Fuchs and M. E. Cates, Phys. Rev. Lett. **89**, 248304 (2002).
- [3] K. Miyazaki and D. R. Reichman, Phys. Rev. E **66**, 050501 (R) (2002).
- [4] L. Berthier, J.-L. Barrat, and J. Kurchan, Phys. Rev. E **61**, 5464 (2000).
- [5] A. Crisanti and H. Sompolinsky, Phys. Rev. A **36**, 4922 (1987).
- [6] H. Horner, Z. Phys. B: Condens. Matter **100**, 243 (1996).
- [7] S. M. Fielding, Phys. Rev. E **66**, 016103 (2002).
- [8] P. Sollich, F. Lequeux, P. Hèbraud, and M. E. Cates, Phys. Rev. Lett. **78**, 2020 (1997).
- [9] F. Thalmann, Eur. Phys. J. B **3**, 497 (1998).
- [10] R. Yamamoto and A. Onuki, Phys. Rev. E **58**, 3515 (1998); R. Yamamoto and A. Onuki, J. Chem. Phys. **117**, 2359 (2002).
- [11] L. Berthier and J.-L. Barrat J. Chem. Phys. **116**, 6228 (2002).
- [12] L. Angelani, G. Ruocco, F. Sciortino, P. Tartaglia, and F. Zamponi, Phys. Rev. E **66**, 061505 (2002).
- [13] D. Bonn, S. Tanase, B. Abou, H. Tanaka, and J. Meunier, Phys. Rev. Lett. **89**, 015701 (2002).
- [14] V. Viasnoff and F. Lequeux, Phys. Rev. Lett. **89**, 065701 (2002).
- [15] G. Petekidis, A. Moussald, and P. N. Pusey, Phys. Rev. E **66**, 051402 (2002).
- [16] A. Mourchid, A. Delville, J. Lambard, E. Lècolier, and P. Levitz, Langmuir **11**, 1942 (1995).
- [17] B. Ruzicka, L. Zulian, and G. Ruocco, Phys. Rev. Lett. **93**, 258301 (2004).
- [18] B. Berne and R. Pecora, *Dynamic Light Scattering* (Wiley, New York, 1976).
- [19] B. J. Ackerson and N. A. Clark, J. Phys. (Paris) **42**, 929 (1981).
- [20] R. Richert, J. Phys.: Condens. Matter **14**, R703 (2002).
- [21] B. Abou, D. Bonn, and J. Meunier, Phys. Rev. E **64**, 021510 (2001).
- [22] D. Bonn, H. Tanaka, G. Wegdam, H. Kellay, and J. Meunier, Europhys. Lett. **45**, 52 (1998).
- [23] H. Tanaka, J. Meunier, and D. Bonn, Phys. Rev. E **69**, 031404 (2004).